International Journal of Nanomedicine

Dovepress
open access to scientific and medical research

Open Access Full Text Article

ORIGINAL RESEARCH

From 3D spheroids to tumor bearing mice: efficacy and distribution studies of trastuzumab-docetaxel immunoliposome in breast cancer

This article was published in the following Dove Press journal:
International Journal of Nanomedicine

Anne Rodallec[1]
Guillaume Sicard[1]
Sarah Giacometti[1]
Manon Carré[1]
Bertrand Pourroy[2]
Fanny Bouquet[3]
Ariel Savina[3]
Bruno Lacarelle[1]
Joseph Ciccolini[1]
Raphaelle Fanciullino[1]

[1]SMARTc Unit, Laboratory of Pharmacokinetics and Toxicology UFR Pharmacy, Center for Research on Cancer of Marseille, Inserm UMR1068, CNRS UMR7258, Aix Marseille University, Marseille, France; [2]Pharmacy Department, APHM La Conception, Marseille, France; [3]Roche Institute, Boulogne Billancourt, France

Purpose: Nanoparticles are of rising interest in cancer research, but in vitro canonical cell monolayer models are not suitable to evaluate their efficacy when prototyping candidates. Here, we developed three-dimensional (3D) spheroid models to test the efficacy of trastuzumab-docetaxel immunoliposomes in breast cancer prior to further testing them in vivo.

Materials and methods: Immunoliposomes were synthesized using the standard thin film method and maleimide linker. Two human breast cancer cell lines varying in Her2 expression were tested: Her2+ cells derived from metastatic site: mammary breast MDA-MB-453 and triple-negative MDA-MB-231 cells. 3D spheroids were developed and tested with fluorescence detection to evaluate viability. In vivo efficacy and biodistribution studies were performed on xenograft bearing nude mice using fluorescent and bioluminescent imaging.

Results: In vitro, antiproliferative efficacy was dependent upon cell type, size of the spheroids, and treatment scheduling, resulting in subsequent changes between tested conditions and in vivo results. Immunoliposomes performed better than free docetaxel + free trastuzumab and ado-trastuzumab emtansine (T-DM1). On MDA-MB-453 and MDA-MB-231 cell growth was reduced by 76% and 25%, when compared to free docetaxel + free trastuzumab and by 85% and 70% when compared to T-DM1, respectively. In vivo studies showed tumor accumulation ranging from 3% up to 15% of the total administered dose in MDA-MB-453 and MDA-MB-231 bearing mice. When compared to free docetaxel + free trastuzumab, tumor growth was reduced by 89% (MDA-MB-453) and 25% (MDA-MB-231) and reduced by 66% (MDA-MB-453) and 29% (MDA-MB-231) when compared to T-DM1, an observation in line with data collected from 3D spheroids experiments.

Conclusion: We demonstrated the predictivity of 3D in vitro models when developing and testing nanoparticles in experimental oncology. In vitro and in vivo data showed efficient drug delivery with higher efficacy and prolonged survival with immunoliposomes when compared to current anti-Her2 breast cancer strategies.

Keywords: docetaxel, trastuzumab, breast cancer, immunoliposome, spheroids, distribution, tumor xenograft

Correspondence: Joseph Ciccolini
SMARTc Unit, UFR Pharmacie
Laboratoire de Pharmacocinétique et Toxicologie, Centre de Recherche en Cancérologie de Marseille, Inserm UMR1068, CNRS UMR7258, Aix-Marseille University, 27 Boulevard Jean Moulin, 13005 Marseille, France
Tel +33 49 183 5541
Email joseph.ciccolini@univ-amu.fr

Introduction

Although widely studied, breast cancer still currently represents the deadliest cancer for women worldwide.[1] Among breast cancer subtypes, the Her2+ ones were once associated with dismal prognostics until the approval in the early 2000's of trastuzumab (Herceptin®), an anti-Her2 monoclonal antibody.[2,3] Combined with taxanes (ie, docetaxel or paclitaxel) it has been approved as first-line treatment for Her2+ patients.[4] Indeed, for metastatic diseases, trastuzumab plus docetaxel largely improved the overall response

submit your manuscript | www.dovepress.com
Dovepress
http://dx.doi.org/10.2147/IJN.S179290

rate (ie, 61% vs 34%, P=0.0002) and overall survival (ie, 31.2 vs 22.7 months, P=0.0325) when compared to docetaxel alone.[4] However, taxanes are characterized by poor solubility requiring the use of toxic excipients triggering neurotoxicities, plus complete lack of specificity toward tumor tissues leading to frequent neutropenia. In this respect, developing nanoparticles-based formulations of docetaxel and paclitaxel could help to improve their pharmacokinetic/pharmacodynamic profile.[5] While protecting the carried drugs, nanoparticles can skip poor solubility issues and improve pharmacokinetics, allowing an excipient-free formulation with greater tumor uptake and lower side effects.[5] Consequently, many liposomes have been studied and have shown remarkable in vitro and in vivo efficacy against a wide range of solid tumors.[5] Our team recently developed a trastuzumab-docetaxel stealth immunoliposome. When first tested in vitro using monolayer models, this immunoliposome proved to perform better than free docetaxel + free trastuzumab.[6] However, and although results were promising, the issue of tumor uptake and tissue diffusion that cannot be properly described with standard two-dimensional (2D) monolayer models makes in vitro efficacy data hardly transposable to in vivo experiments. Indeed, only three-dimensional (3D) models better mimicking cell–cell junctions, cell–matrix interactions, cell polarity, and oxygen gradient can closely predict biological responses, provided that the right culturing conditions are met.[7,8] Spheroids are 3D structures made of aggregated cells exhibiting tissue organization, metabolic characteristics, and specialized functions.[7] Moreover, these models can be cultured for a longer period (ie, several weeks) and therefore be exposed to prolonged and repeated treatments, thus better adhering to future in vivo conditions.[7] However, they need to be cautiously adapted and validated for each cell line and applications.[9] To date, few 3D models have been published to test immunoliposomes in vitro, canonical monolayer cell models remaining the mainstay in experimental oncology. The purpose of this study was therefore to develop tumor spheroids using cells derived from metastatic site: mammary breast (MDA-MB)-231 and MDA-MB-453 breast cancer cells, to set up the right culture conditions so as to test our prototype of trastuzumab-docetaxel stealth immunoliposome. In vivo experiments were next performed in mice orthotopically xenografted with MDA-MB-231 and MDA-MB-453 so as to confirm the relevance of the 3D model to predict in vivo efficacy.

Materials and methods

Cell lines

Experiments were carried out on two human breast cancer cell lines: MDA-MB-453 (Her2+) and MDA-MB-231 (Her2−). Cells were purchased from the American Type Culture Collection (Manassas, VA, USA). They were cultured in Roswell Park Memorial Institute (RPMI) medium supplemented with 10% FBS, 50,000 UI/L penicillin, 50,000 µg/L streptomycin, and 16,000 µg/L kanamycin and grown in a humidified CO_2 incubator at 37°C. Cell lines were stably transfected with dTomato lentivirus developed and kindly provided by Pr Jacques Robert, Institut Bergonié, Bordeaux, France and selected with blasticidin to allow fluorescence imaging if required. These lines were further infected with firefly luciferase (Luc+) and selected with puromycin (PerkinElmer Inc, Waltham, MA, USA). Cells were regularly authenticated on cell viability, morphology, and doubling time.

Drugs and chemicals

Egg yolk phosphatidylcholine (PC), phosphatidylglycerol (PG), cholesterol (Chol), 1,2-distearoyl-*sn*-glycero-3-phosphoethanolamine, and paclitaxel were purchased from Sigma-Aldrich Co (St Louis, MO, USA). 1,2-Distearoyl-*sn*-glycero-3-phosphoethanolamine-N-[maleimide (polyethylene glycol)]-2000 (Mal-PEG) was purchased from Coger (Paris, France). Docetaxel was purchased from VWR International (Fontenay-sous-Bois, France). DiR and DiL fluorophore tags were purchased from PerkinElmer Inc and Thermo Fisher Scientific (Waltham, MA, USA). 2-Iminothiolane (Traut's reagent) was also purchased from Thermo Fisher Scientific. Trastuzumab was kindly provided by Genentech (South San Francisco, CA, USA). All other reagents were of analytical grade.

Immunoliposome preparation

As previously described, liposomes were synthesized using the thin film method.[6] PC, Chol, PG, docetaxel, and Mal-PEG were mixed in a 50:19:15:1.7:1 molar ratio. Briefly, lipids were dissolved in methanol. The lipid solution was further mixed with DiR or DiL as fluorophore when required. Methanol was then removed by rotary evaporation (Laborota 4003; Heidolph Instruments, Schwabach, Germany) at 38°C. After 30 minutes a thin lipid film was obtained. To remove the remaining solvent, this lipid film was dried under a stream of nitrogen for 2 hours at room temperature. The film was then hydrated with a 5% v/v glucose solution, and large liposomes were obtained. Reduction and homogenization in size were thus achieved by extrusion using a LipoFast LF-50, through 100 and 80 nm polycarbonate pore membranes (Nucleopore; Whatman®, Little Chalfont, Maidstone, UK) with two cycles per pore size. Trastuzumab was then engrafted using a maleimide linker and requiring a preliminary step of trastuzumab

thiolation.[10,11] Trastuzumab was first dissolved in a 0.1 M sodium phosphate buffer (PBS) pH 8.0, containing 5 mM EDTA and mixed under constant shaking, for 2 hours at room temperature with a Traut's reagent solution at 1:10 molar ratio (Traut's:trastuzumab). Thiolated trastuzumab was then directly mixed with the pegylated liposomes at 1:127 molar ratio (trastuzumab:Mal-PEG). The mixture was kept under constant shaking at 4°C overnight. Unbound trastuzumab and free docetaxel were removed using 6,000×*g* centrifugation on MWCO 300 kDa Vivaspins (VWR International) and exclusion chromatography on qEV columns (Izon Science, Christchurch, New Zealand).

Size and polydispersity determination

Size and polydispersity index (PDI) were measured by dynamic light scattering. Liposomes and immunoliposomes were diluted in PBS solution and then analyzed by a Zetasizer Nano S (Malvern Instruments, Malvern, UK). Liposomal preparations were considered unimodal with PDI <0.2.[12]

Measurement of docetaxel and trastuzumab concentrations

Docetaxel concentration was measured using HPLC-ultraviolet (UV) method after liquid/liquid extraction using a C18 column (25 cm ×4.6 mm, 5 µm; Waters Corporation, Milford, MA, USA).[13] The mobile phase was composed of 53% of an ammonium acetate buffer (35 nM, pH 5) and 47% of acetonitrile. Samples were eluted at a constant flow rate of 1.8 mL/min with UV detection (227 nm). Data were acquired and analyzed using ChemStation software (Agilent Technologies, Santa Clara, CA, USA). Docetaxel and paclitaxel typical retention times were, respectively, 11 and 13.5 minutes.

Trastuzumab engraftment rate

Trastuzumab was indirectly measured by Bradford assay, using thiolated trastuzumab as a standard.[14]

Stability studies

Stability studies were previously performed in PBS at 4°C, protected from light.[6] Docetaxel leakage from immunoliposomes and liposomes was also evaluated in biological environment using RPMI culture media (Thermo Fisher Scientific) at 37°C, after 5 minutes, 30 minutes, 1 hour, 24 hours, and 1 week incubation with gentle stirring.

In vitro cytotoxicity studies

Spheroids were obtained using dTomato+ MDA-MB-453 and MDA-MB-231 seeded with 20% methylcellulose solution on U-bottom 96-well plates for 24 hours before the experiment. To evaluate antiproliferative efficacy of the treatment on spheroids, the following conditions were tested: spheroids size (low-density seeding, high-density seeding) and drug concentrations (low [IC50], high [4× IC50]). Additionally, two different scheduling were tested on small size spheroids: early incubation (ie, D3, D10) and delayed incubation (ie, D6, D13). Because spheroid morphology and fluorescence were cell line specific, cell density was 1,500 and 4,000 cells/well for MDA-MB-453 and 10,000 and 25,000 cells for MDA-MB-231. After 3 or 6 days, cells were exposed continuously to drugs for 1 week, then treatment was repeated, and drugs incubated until day 14. Different conditions were tested: free docetaxel + free trastuzumab, liposomes + free trastuzumab, immunoliposomes, and ado-trastuzumab emtansine (T-DM1). Drug concentrations (low and high) were docetaxel 2 and 8 nM, trastuzumab 4 and 16 pM, regardless of the form (ie, free drug or liposomal). T-DM1 concentration was 3.25 and 13 ng/mL. Cell viability was determined using cell fluorescence and spectrophotometric reading at 580/620 nm (PHERAstar FSX;® BMG Labtech, Ortenberg, Germany). Spheroids were also monitored daily using a fluorescence microscope (Eclipse TS100; Nikon Corporation, Tokyo, Japan), coupled to a digital camera.

In vivo efficacy studies

Antitumor efficacy was tested in MDA-MB-453 and MDA-MB-231 bearing mice. Briefly, 6-week-old female nude mice (Charles River, France; n=86) were orthotopically grafted (mammary fat pad) with 80,000 MDA-MB-453 or MDA-MB-231 cells in 60% Matrigel. After 18 days, mice were divided in five groups: control (saline), free docetaxel + free trastuzumab, liposomal docetaxel + free trastuzumab, immunoliposomes, or T-DM1. All treatments were administered intraperitoneally once a week over 6 consecutive weeks. Docetaxel and trastuzumab were administered at 5 and 1.9 mg/kg, respectively, either when given as free drugs or as immunoliposome. T-DM1 dose was 10 mg/kg. For the MDA-MB-231 model, tumor growth was initially monitored by fluorescence imaging. However, because of a loss in dTomato expression in vivo, mid-study we shifted to volumetric measurements using a vernier caliper. Tumor growth was monitored twice a week. With MDA-MB-453 xenografts, tumor growth was measured directly using a caliper from the beginning of the experiment. After 50 days, 3D bioluminescence analysis was performed to evaluate metastatic spreading. All imaging was performed using an IVIS Spectrum

imager equipped with Living Image 4.2.1 software (PerkinElmer Inc).

In vivo distribution studies

Biodistribution studies were performed weekly, after using DiR-labeled nanoparticles with subsequent imaging in MDA-MB-453 and MDA-MB-231 bearing mice. Imaging was performed on an IVIS Spectrum imager equipped with Living Image 4.2.1 software. DiR-labeled nanoparticles were excited at 745 nm and emission was recorded from 780 to 840 nm. Tumor targeting was evaluated by measuring the relative amount of DiR-related fluorescence in the tumor vs whole body fluorescence.

Blood vessel density was evaluated at the beginning and end of treatment on three satellite mice using the AngioSense kit (PerkinElmer Inc). AngioSense® 680 EX (100 µL) was administered via tail vein injection and imaging was performed on an IVIS Spectrum imager equipped with Living Image 4.2.1 software 24 hours postinjection.

Statistical analysis

In vitro experiment was performed at least in triplicate and data are represented as mean ± SD or ± standard error of the mean. Statistical analyses were performed on SigmaStat (Systat Software, San Jose, CA, USA). Differences between treatments were analyzed by one-way ANOVA with Newman–Keuls multiple comparison testing or Student's *t*-test according to the data distribution and sample size.

Animal ethics

Guidelines for animal welfare in experimental oncology as recommended by European regulations (decree 2013-118 of February 1, 2013) were followed. All animal experiments were approved by the Animal Ethic Committee of the Aix-Marseille Université (CE14). The protocol was registered as #2017031717108767 at the French Ministry of Research. Mice were monitored daily for signs of distress, pain, decreased physical activity, or any behavioral change and weighted thrice a week. Water was supplemented with paracetamol (80 mg/kg/day) to prevent any metastasis-related pain.

Results

Immunoliposome characterization

Immunoliposome population was unimodal (PDI =0.1±0.01) with a 140±3.4 nm diameter. Docetaxel encapsulation efficiency was >90% and trastuzumab engraftment efficiency was 31%±6%.

Stability studies

When kept in RPMI culture media at 37°C, after 5 minutes, 18% and 27% (P=0.321, Student's t-test) of docetaxel leaked from liposomes and immunoliposomes (Figure 1). After stabilization, docetaxel leakage was similar to the PBS matrix condition previously published.[6]

In vitro cytotoxicity studies

Empty liposomes and trastuzumab alone did not show cytotoxic effect on our two cell models (data not shown). Results of the cytotoxicity assays are shown in Figures 2 and 3. To avoid listing out numerous data obtained, the examples given in this paragraph pertain to high concentrations only (ie, [docetaxel] =8 nM, [trastuzumab] =16 pM,

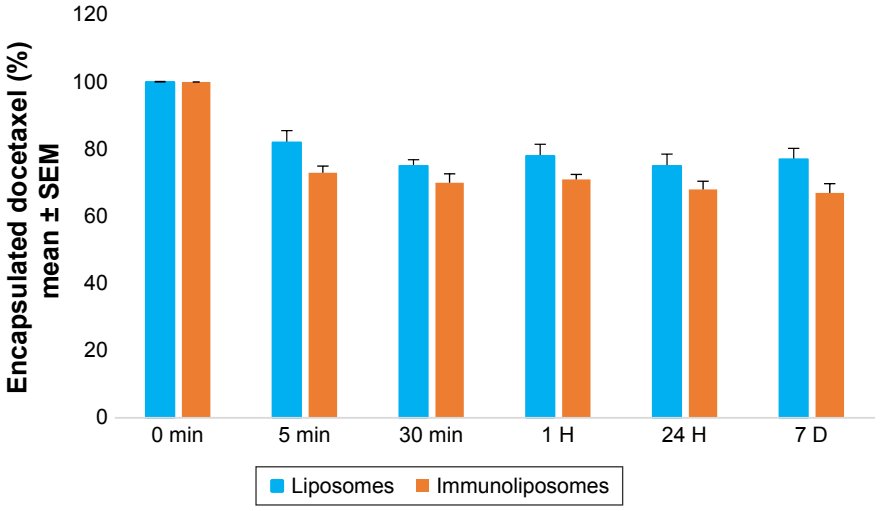

Figure 1 Monitoring of docetaxel encapsulated in liposomes or immunoliposome (%) kept in biological environment (ie, RPMI) at 37°C, over time.[a]
Note: [a]Values are mean ± SEM of three or more experiments.
Abbreviations: SEM, standard error of the mean; RPMI, Roswell Park Memorial Institute medium.

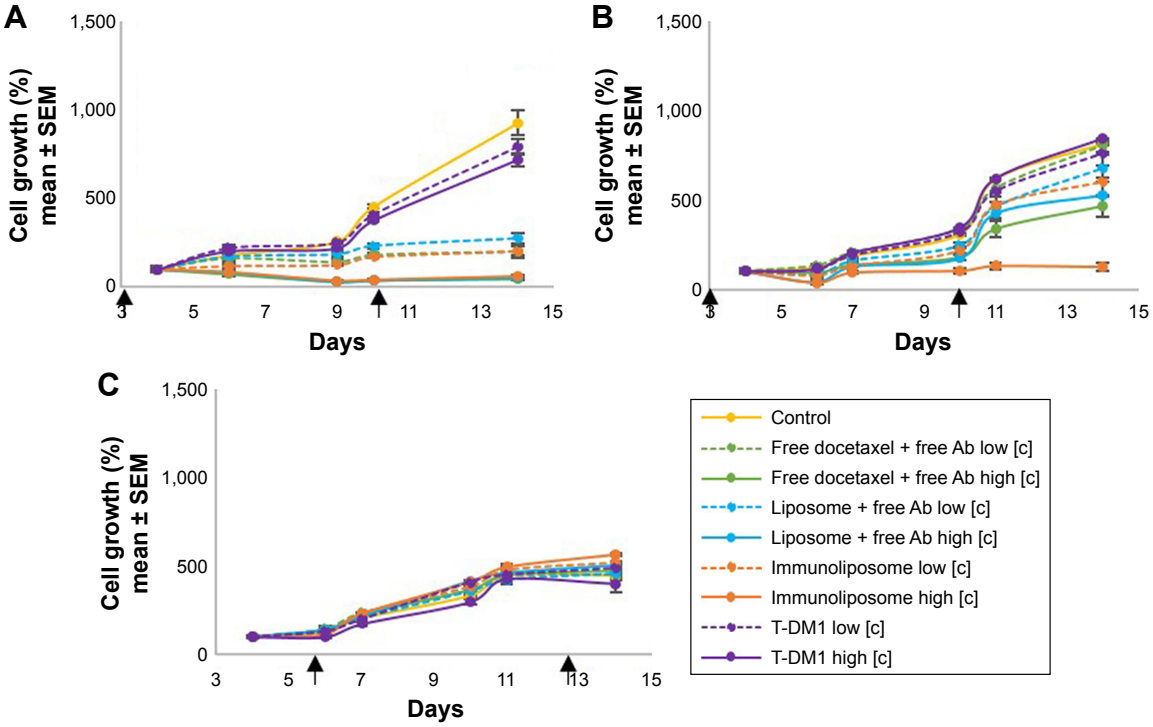

Figure 2 MDA-MB-453 growth monitoring on 3D spheroids models. Spheroids were seeded with 1,500 cells (**A**, **C**) or 4,000 cells (**B**) and treated with free docetaxel + free trastuzumab, liposomes + free trastuzumab, immunoliposomes, or T-DM1 at low concentration (ie, [docetaxel] =2 nM, [trastuzumab] =4 pM, and [T-DM1] =3.25 ng/mL) and high concentration (ie, [docetaxel] =8 nM, [trastuzumab] =16 pM, and [T-DM1] =13 ng/mL), at day 3 and day 10 (**A**, **B**) or day 6 and day 13 (**C**).[a]
Notes: [a]Values are mean ± SEM of three or more experiments. The square brackets refer to the concentration.
Abbreviations: SEM, standard error of the mean; 3D, three-dimensional; T-DM1, ado-trastuzumab emtansine; MDA-MB, derived from metastatic site: mammary breast; Ab, trastuzumab.

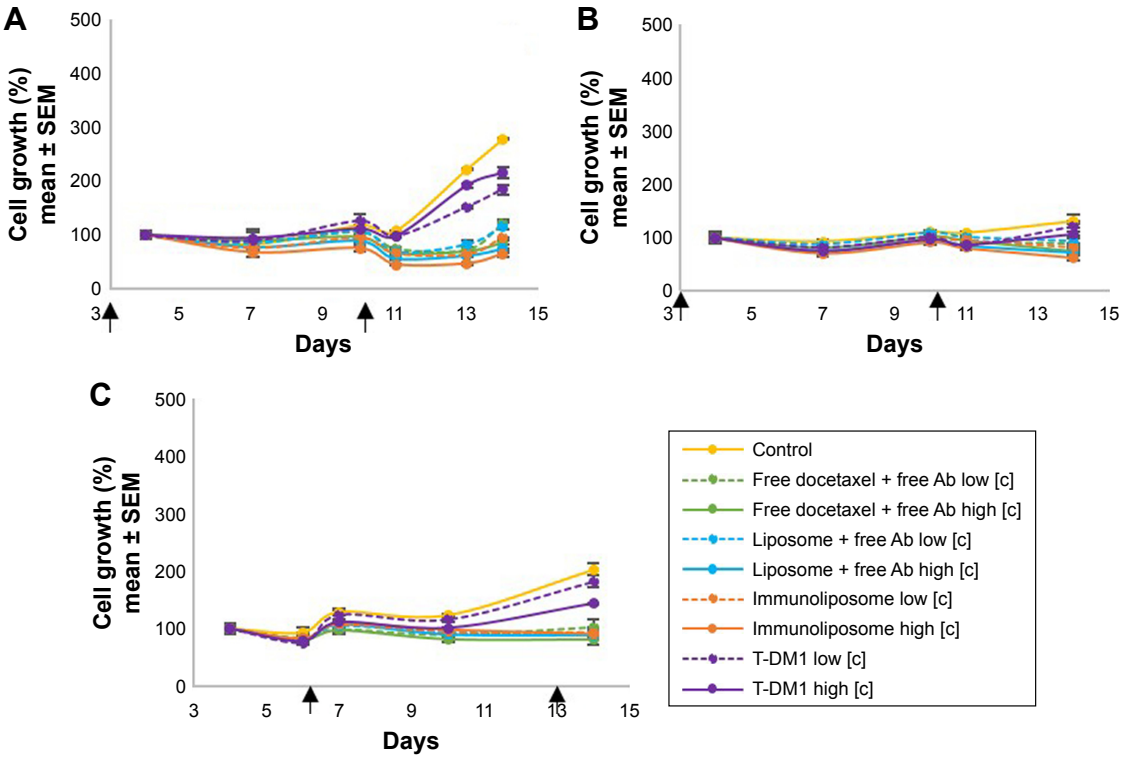

Figure 3 MDA-MB-231 growth monitoring on 3D spheroids models. Spheroids were seeded with 1,000 cells (**A**, **C**) or 25,000 cells (**B**) and treated with free docetaxel + free trastuzumab, liposomes + free trastuzumab, immunoliposomes, or T-DM1 at low concentration (ie, [docetaxel] =2 nM, [trastuzumab] =4 pM, and [T-DM1] =3.25 ng/mL) and high concentration (ie, [docetaxel] =8 nM, [trastuzumab] =16 pM, and [T-DM1] =13 ng/mL) at day 3 and day 10 (**A**, **B**) or day 6 and day 13 (**C**).[a]
Notes: [a]Values are mean ± SEM of three or more experiments. The square brackets refer to the concentration.
Abbreviations: SEM, standard error of the mean; 3D, three-dimensional; T-DM1, ado-trastuzumab emtansine; MDA-MB, derived from metastatic site: mammary breast; Ab, trastuzumab.

and [T-DM1] =13 ng/mL; with the square brackets denoting concentration) at the end of the study (ie, 14 days).

On MDA-MB-453 low-density spheroids, early incubation led to concentration-dependent cytotoxicity (Figure 2A); the higher the concentration, the higher the antiproliferative effect. Free drugs, docetaxel liposomes + free trastuzumab, and immunoliposomes showed marked efficacy as cell growth was reduced by 95%, 94%, and 94% when compared to the control group, respectively, but no difference was observed between treatments (P=0.599, one-way ANOVA with multiple comparison testing). T-DM1 performance was significantly lower than other treatments because cell growth was reduced by 23% only (P<0.001, one-way ANOVA with multiple comparison testing). When seeded at higher density, we observed an increase in the efficacy with immunoliposomes (Figure 2B). When compared to the control group, free docetaxel + free trastuzumab and liposomes + free trastuzumab performed equally (ie, cell growth reduction of 43%, 35%, P=0.892, Student's t-test), whereas immunoliposomes showed significantly higher efficacy (ie, cell growth reduction 85%, P=0.041, one-way ANOVA). T-DM1 had still no effect (P=0.632, Student's t-test vs control). With delayed incubation on low-density spheroids, antiproliferative efficacy was no longer observed (P=0.326, one-way ANOVA), regardless of the treatments, with respect to control (Figure 2C).

On MDA-MB-231 low-density spheroids, early incubation led to concentration-dependent cytotoxicity (Figure 3A). Both liposomal forms performed slightly better than the other drugs. When compared to control, cell growth reduction was 69%, 73%, 77%, and 22% (P<0.001, one-way ANOVA with multiple comparison testing) for free drugs, docetaxel liposomes + free trastuzumab, immunoliposomes, and T-DM1 groups, respectively. When seeded at higher density we observed similar results (Figure 3B) as cell growth was reduced significantly by 43%, 46%, 53%, and 19% (P<0.001, one-way ANOVA), respectively. With delayed incubation on low-density spheroids (Figure 3C), free drugs, docetaxel liposomes + free trastuzumab, and immunoliposomes showed equal efficacy as cell growth was reduced by 60%, 56%, and 55% when compared to the control group, respectively, and no difference was found between treatments (ie, P>0.05, one-way ANOVA with multiple comparison testing). T-DM1 performance was significantly lower as cell growth was reduced by 29% only (P=0.017, one-way ANOVA with multiple comparison testing).

In vivo distribution studies

Figure 4 shows typical fluorescence after spectral unmixing, allowing to localize and to quantify separately DiR-labeled nanoparticles into tumors. With MDA-MB-453 xenografts, both at the end of the treatment (ie, D51) and mid-study (ie, D67), 1%±1% of the administered immunoliposomes accumulated in the tumor (Figure 5A). With liposomes, 1%±1% and 4%±3% were found in tumors at D51 and D67, respectively. However, no significant difference was observed between immunoliposomes and liposomes intratumor accumulation throughout time (P>0.05, Student's t-test).

For MDA-MB-231 cell line, at the end of the treatment (ie, D51) and the end of the study (ie, D67), 11%±10% and

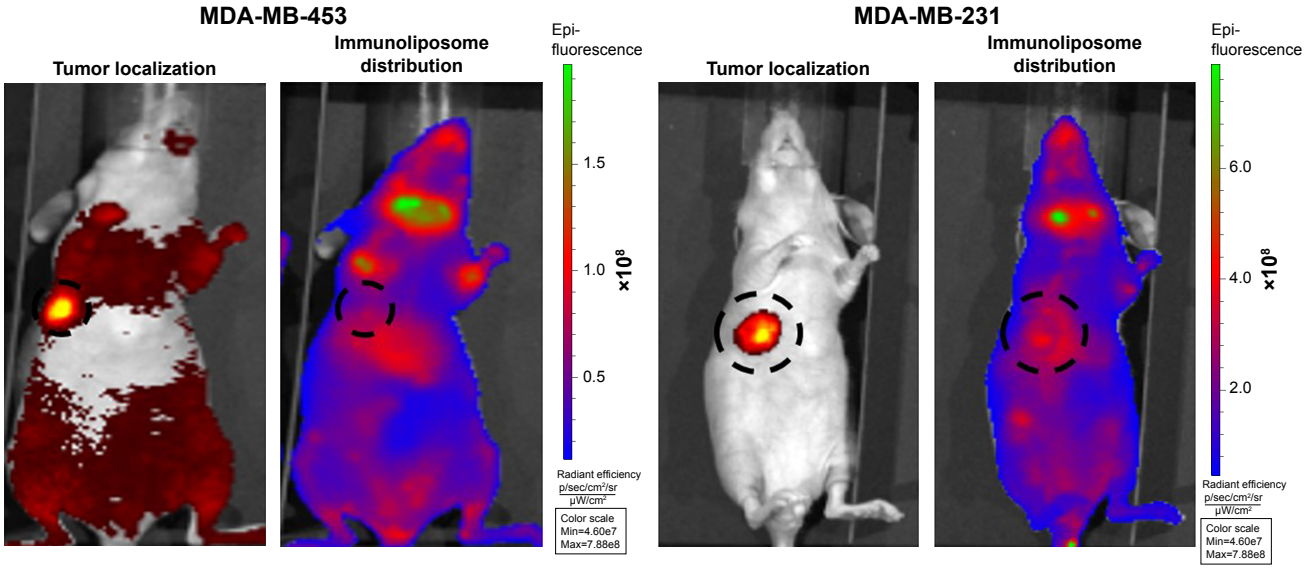

Figure 4 Spectral unmixing of dTomato+ MDA-MB-453 and MDA-MB-231 bearing mice, 5 days after administration of DiR-labeled immunoliposomes.
Abbreviation: MDA-MB, derived from metastatic site: mammary breast.

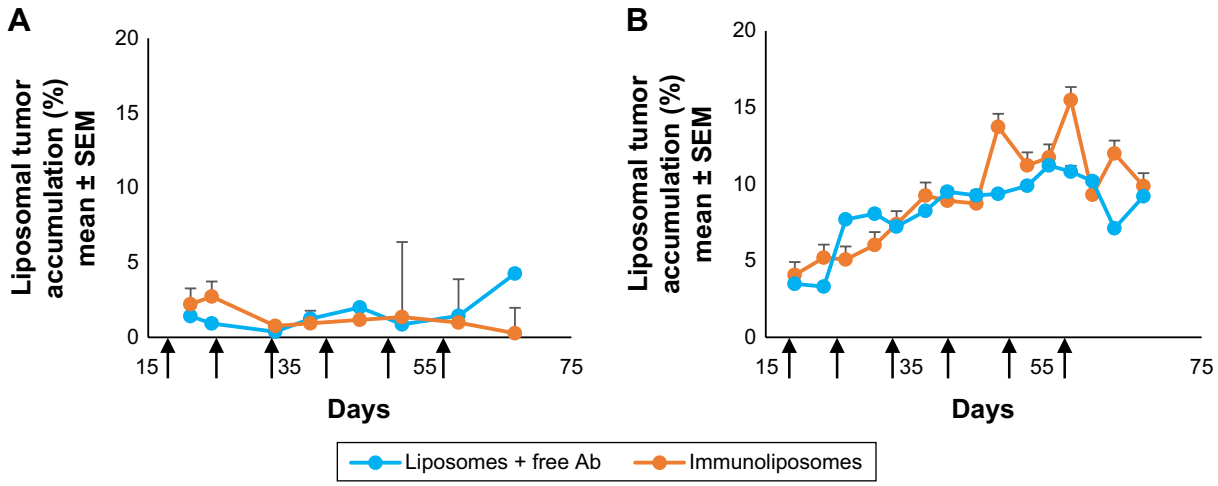

Figure 5 Accumulation of liposomes and immunoliposomes in the tumor: monitoring of the relative fluorescence measured in tumors (%) as compared with whole body fluorescence.
Note: Accumulation in (**A**) MDA-MB-453 tumor and (**B**) MDA-MB-231 tumor (n≥7 per group).
Abbreviations: SEM, standard error of the mean; MDA-MB, derived from metastatic site: mammary breast; Ab, trastuzumab.

10%±1% of the administered immunoliposomes accumulated in the tumor (Figure 5B). Similarly, 10%±2% and 9%±1% of the liposomes were found in the tumor. No significant difference was observed again between immunoliposomes and liposomes intratumor accumulation throughout time ($P>0.05$, Student's *t*-test).

As shown in Figure 6 and Table 1, tumor vascularization was found to increase over time. In the control group, at the beginning of the treatment, MDA-MB-453 and MDA-MB-231 were found to be similarly vascularized (ie, 1.15×10^{10} photons/s vs 1.19×10^{10} photons/s, $P=0.929$, Student's *t*-test). However, at the end of the treatment, MDA-MB-453 cells were found to be less vascularized than the MDA-MB-231 model (ie, 1.73×10^{10} photons/s vs 5.96×10^{10} photons/s, $P<0.05$, Student's *t*-test). In MDA-MB-453 bearing mice, at the end of the treatment, tumor vascularization showed 50% and 188% increase for control and liposomes + free trastuzumab groups, respectively. This increase was only up to 1% for immunoliposomes ($P=0.079$, one-way ANOVA). For MDA-MB-231 bearing mice, at the end of the treatment, tumor vascularization showed a 401% increase for the control group, while liposomes + free trastuzumab and immunoliposomes displayed increases to 160% and 149% only, respectively ($P=0.206$, one-way ANOVA).

In vivo efficacy studies

Regardless of the treatment, no toxicity was observed in mice (data not shown) and no difference in carcass weight was observed (data not shown). Empty liposomes administered to mice showed no effect on tumor size throughout time (data not shown).

Figure 7 shows tumor growth on MDA-MB-453 bearing mice. At the end of the study, all treatments (ie, free drugs, liposomes + free trastuzumab, immunoliposomes, or T-DM1) showed near-complete efficacy on tumor size (ie, at end of the study, tumor size was reduced by 99%, 100%, 100%, and 100% when compared to the control group, respectively). When comparing treatments to free docetaxel + free trastuzumab, tumor size was reduced by 68%, 77%, and 89% for T-DM1, docetaxel liposomes + free trastuzumab, and immunoliposomes, respectively. One-way ANOVA testing showed a significant difference between treatments ($P=0.003$). At the end of the study, survival was 100% for all groups (data not shown). No metastasis was observed by bioluminescence imaging in MDA-MB-453 mice (Figure 8).

Figure 9 shows tumor growth on MDA-MB-231 bearing mice. At the end of the study (ie, D67), tumor size failed to reduce when treated with free drugs, liposomes + free trastuzumab, and T-DM1 (ie, 5%, 5%, and 0% reduction, respectively, $P=0.720$, one-way ANOVA), whereas the immunoliposomes group presented a significant 28% decrease in tumor size ($P=0.031$, Student's *t*-test). Similarly, at the end of the study (ie, D67), when compared to T-DM1, only the immunoliposome group reduced tumor size (ie, 29% reduction, $P=0.041$, Student's *t*-test). Although not significant (ie, $P>0.05$, Student's *t*-test), a reduction of 24% was observed when compared to free drugs. Main metastatic sites in MDA-MB-231 mice were liver, bone, and lung (Figure 8). At mid-treatment, at least one metastatic site was found in 66%, 100%, 33%, 66%, and 100% of the control, free drugs, docetaxel liposomes + free trastuzumab, immunoliposomes, and T-DM1 groups; all animals demonstrated metastasis at the end of the

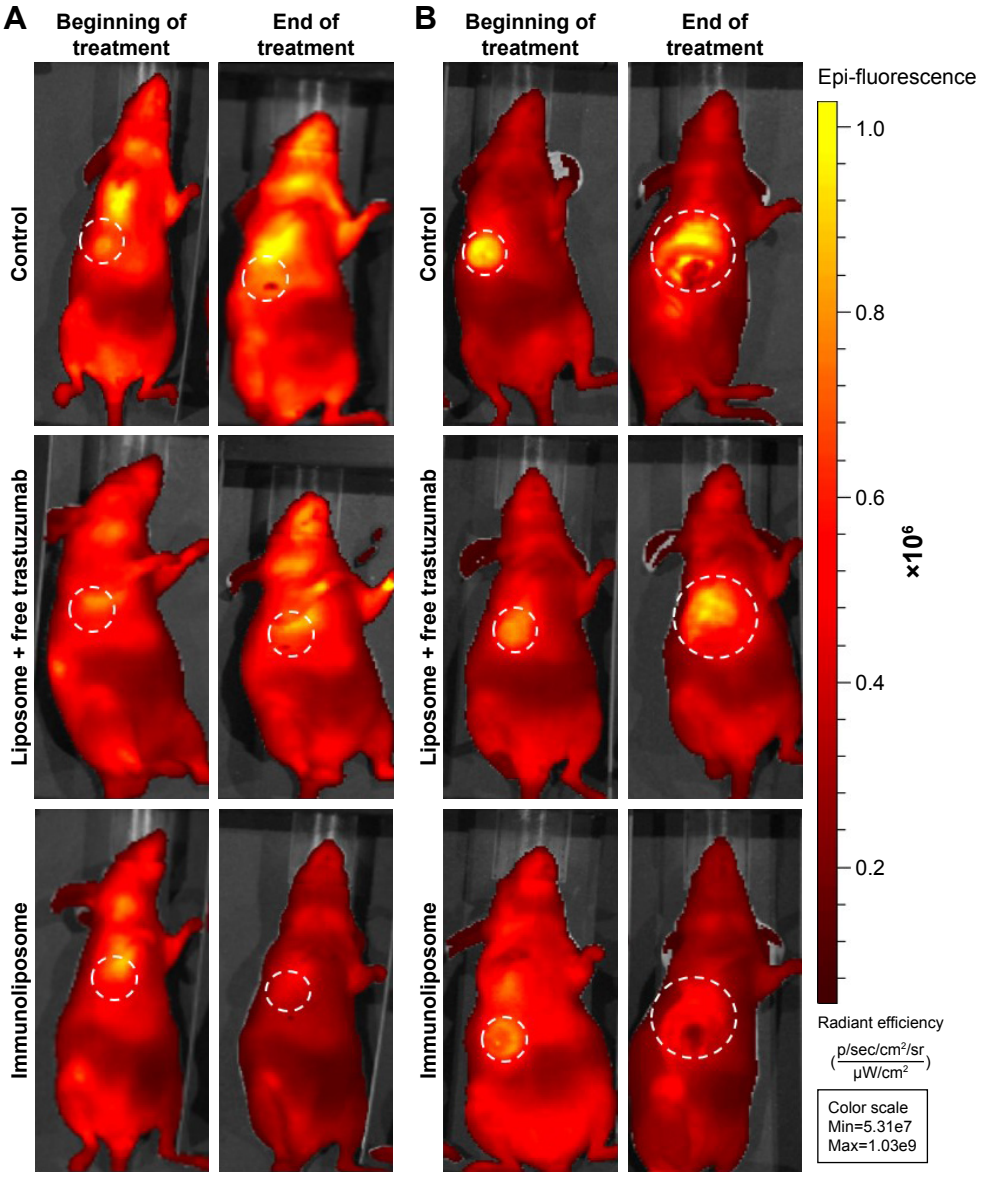

Figure 6 Vascularization fluorescence of control, liposome + free trastuzumab, and immunoliposome groups of MDA-MB-453 (**A**) and MDA-MB-231 (**B**) bearing mice, 24 hours after AngioSense administration (n≥3 per group).
Abbreviation: MDA-MB, derived from metastatic site: mammary breast.

Table 1 Vascularization fluorescence (photons/s) measured with AngioSense kit on MDA-MB-453 and MDA-MB-231 bearing mice (n≥3 per group)

Treatment	Beginning of treatment ($\times 10^{10}$)	End of treatment ($\times 10^{10}$)
MDA-MB-453 bearing mice		
Control	1.15	1.73
Liposome + free trastuzumab	8.77	2.53
Immunoliposome	1.70	1.72
MDA-MB-231 bearing mice		
Control	1.19	5.96
Liposome + free trastuzumab	1.49	3.88
Immunoliposome	1.38	3.44

Abbreviation: MDA-MB, derived from metastatic site: mammary breast.

treatment. Survival data are summarized in Figure 10. At the end of the study, survival was 0% (control), 0% (free docetaxel + free trastuzumab), 0% (T-DM1), 10% (liposomes + free trastuzumab), and 33% (immunoliposomes).

Discussion

In HER2+ breast cancer, T-DM1 (Kadcyla®) has been the first antibody–drug conjugate to be approved, thus illustrating how optimizing drug delivery was an ongoing issue in clinical oncology.[15] Via passive enhanced permeation and retention (EPR) effect and/or the use of actively targeting agents, nanoparticles are expected to better accumulate in tumors[16] and optimize drug delivery while limiting exposure to healthy tissues.[17] In this context, we developed a new

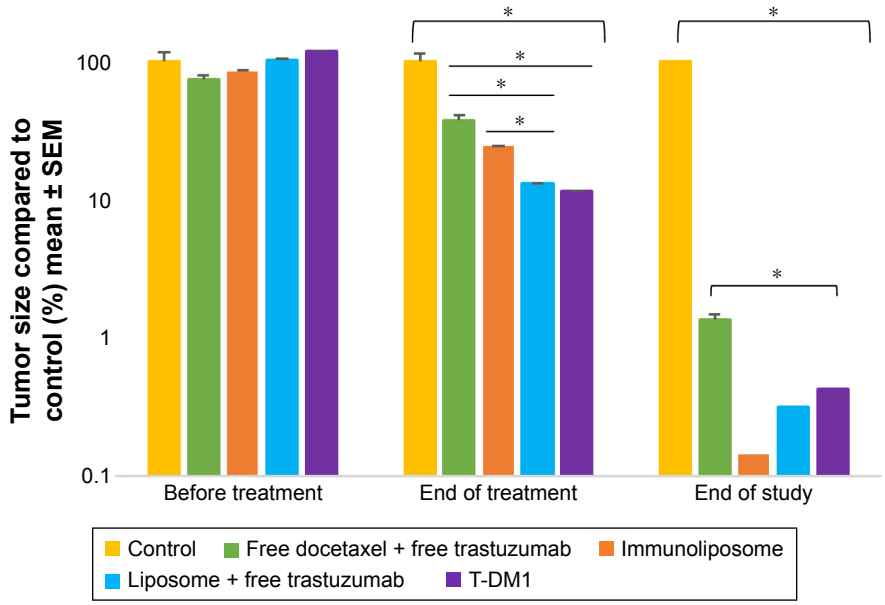

Figure 7 Monitoring of tumor size of MDA-MB-453 bearing mice, measured with caliper (n≥7 per group).
Note: *$P<0.05$.
Abbreviations: SEM, standard error of the mean; T-DM1, ado-trastuzumab emtansine; MDA-MB, derived from metastatic site: mammary breast; Ab.

immunoliposome combining docetaxel and trastuzumab, the latter being used both as a targeting and a therapeutic agent in breast cancer. This new entity showed promising features such as optimal size (ie, <150 nm), high docetaxel encapsulation rate (ie, >90%), and trastuzumab engraftment rate (ie, >30%).[6] In vitro efficacy studies were previously performed on 2D monolayer assays, on a limited but representative panel of human breast cancer cells (ie, MDA-

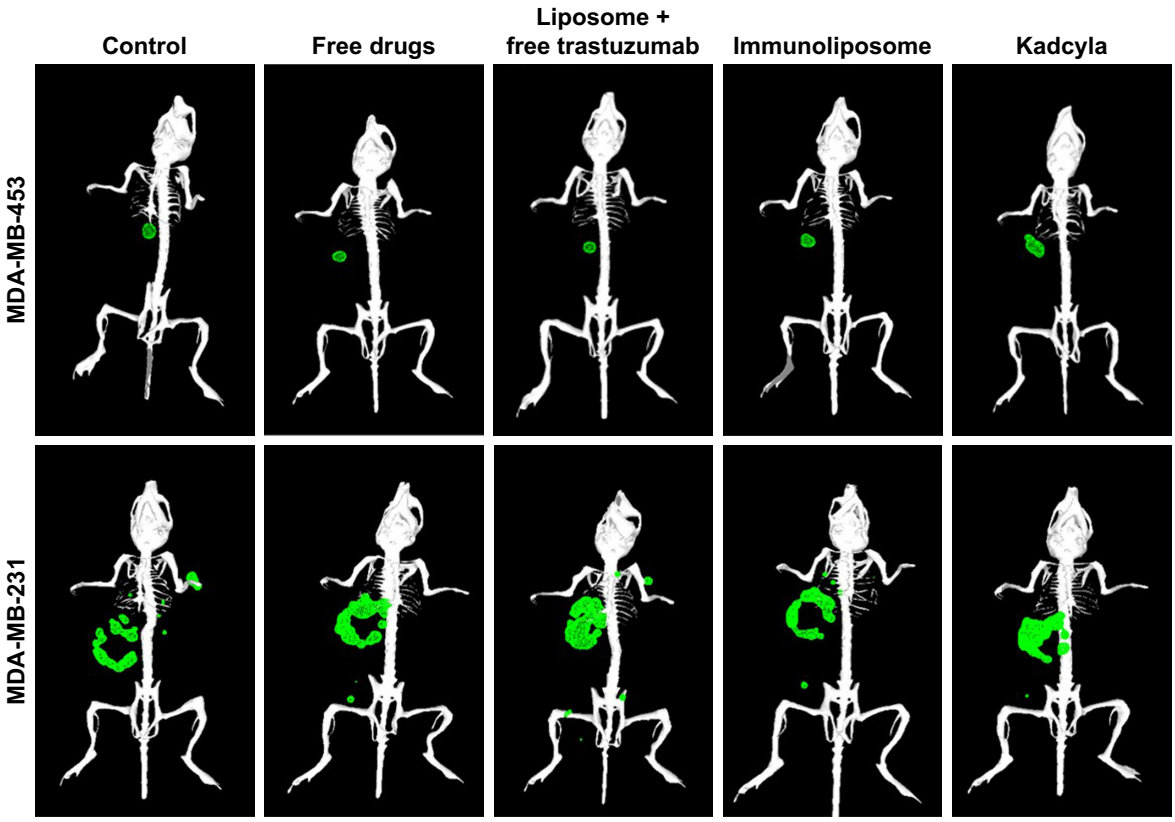

Figure 8 3D reconstruction of MDA-MB-453 and MDA-MB-231 bearing mice.
Note: Primary tumors (●) and metastasis (●) were observed by bioluminescence 50 days after tumor engraftment (n≥3 per group).
Abbreviations: MDA-MB, derived from metastatic site: mammary breast; 3D, three-dimensional.

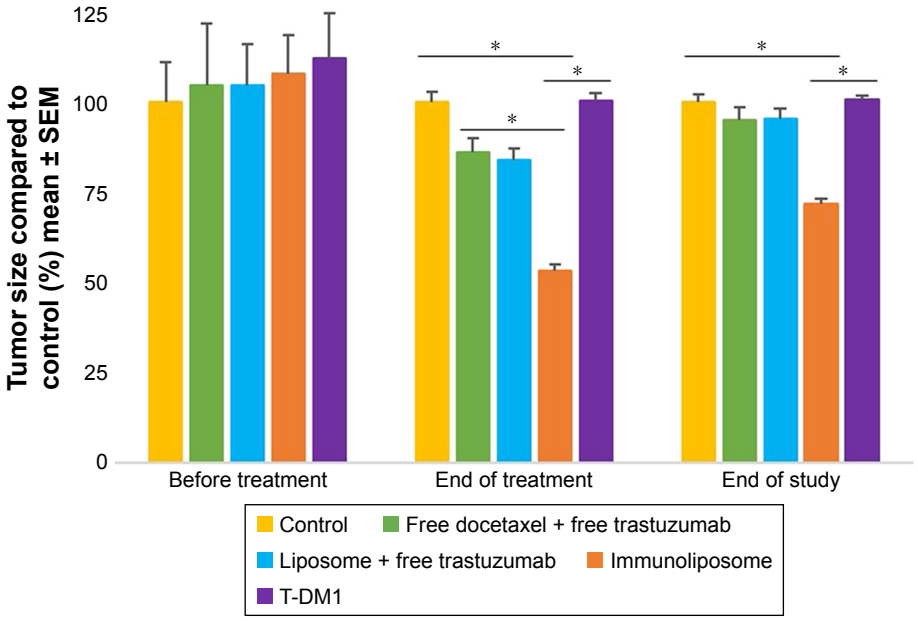

Figure 9 Monitoring of tumor size of MDA-MB-231 bearing mice, measured with caliper (n≥7 per group).
Note: *$P<0.05$.
Abbreviations: SEM, standard error of the mean; T-DM1, ado-trastuzumab emtansine; MDA-MB, derived from metastatic site: mammary breast.

MB-453 and MDA-MB-231) with little differences between treatments.[6] We then hypothesized that 2D monolayer models were not suitable to actually evaluate the antiproliferative efficacy of nanoparticles and that better mimicking tumor organization and microenvironment were necessary. To this end, we developed 3D spheroid models. Cell viability and proliferation are usually evaluated with standard colorimetric methods (eg, MTT reagent, alamarBlue®) or measurement of spheroid diameter.[18–20] However, whereas measuring size lacks specificity, the tight cell–cell junction prevents proper uptake of standard dyes into the spheroids core.[7] Thus, we used dTomato-transfected cells and fluorescence detection to evaluate cell viability. Importantly, we found that the antiproliferative efficacy was dependent upon culture conditions of the spheroids, and that these conditions varied depending on the cell lines considered. This observation is in line with previous reports showing that spheroids features (size, density, incubation time) may greatly impact subsequent efficacy results, because of changes in cell–cell junctions and cell–matrix junction.[9,21] Here, immunoliposomes proved to perform better than all other treatments, including Her2-negative MDA-MB-231 cells. Conversely, T-DM1 failed to exhibit any antiproliferative efficacy in vitro. Of note, the spheroids used in our experiments were only mono-cells and one can hypothesize that improperly mimicking the complexity of the tumor micro-environment could possibly impair the efficacy of antibody–drug conjugates. Still, to the best of our knowledge, this is the first time that comparative in vitro data are reported with T-DM1. In vivo results confirmed the superiority of immunoliposomes over all other treatments, including T-DM1. Surprisingly, this was observed for triple-negative MDA-MB-231 cells as well. Several hypotheses can be used to explain this efficacy despite the lack of highly expressed targets in MDA-MB-231. First, we previously showed that Her2 expression was not entirely abrogated in MDA-MB-231,[6] thus enabling at least partly active targeting by trastuzumab. However, the fact that T-DM1 failed to exhibit any efficacy with MDA-MB-231 either in vitro or in vivo, makes this hypothesis not highly convincing. A second hypothesis is that immunoliposomes have benefited from the EPR effect, enabling nanoparticles to accumulate because of their adequate diameter.[16,22] This is supported by the fact that the vascular density was particularly high in MDA-MB-231 xenografts, and we have demonstrated previously that

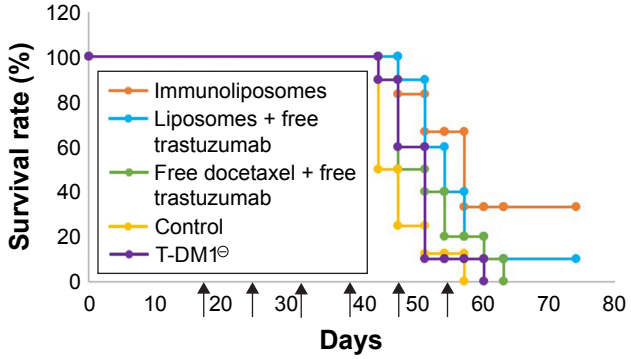

Figure 10 Survival curve of MDA-MB-231 bearing mice (n≥7 per group).
Note: ↑: Cycle starts.
Abbreviations: T-DM1, ado-trastuzumab emtansine; MDA-MB, derived from metastatic site: mammary breast.

the higher the density, the higher the tumor uptake and the efficacy.[23] Here, tumor uptake of immunoliposomes was up to 15% of the total dose recovered in MDA-MB-231 bearing mice, probably explaining the remarkable antiproliferative efficacy we observed. With Her2 expressing MDA-MB-453 xenografts, both immunoliposomes and T-DM1 exhibited significant efficacy in vivo, with immunoliposomes performing better than T-DM1. In this case, the superiority of the immunoliposome could come from the differences in lipophilicity between T-DM1 and the lipidic carrier. As an IgG, trastuzumab is characterized by a low Log *P*-value, rendering passage through biological membranes and diffusion toward tumor tissues particularly challenging with a limited volume of distribution and transporter-dependent extravasation out of the vascular space. Conversely, immunoliposomes can extravasate more easily through the EPR effect, and high lipophilicity ensures higher and more rapid diffusion throughout tissues, including the targeted tumors. Consequently, the in vivo efficacy of T-DM1 was probably due to high basal Her2 expression in this model, whereas the efficacy of the immunoliposomes was more likely to be due to a combined effect of anti-Her2 targeting and EPR effect. This combined effect also explains probably why immunoliposomes performed better than docetaxel liposome associated with free trastuzumab. Although tumor accumulation was found to be similar for immunoliposomes and liposomes, Kirpotin et al demonstrated higher tumor cell internalization with immunoliposomes than liposomes, thus explaining better performance.[24] We observed that vascular density was lower in MDA-MB-453 than in MDA-MB-231 xenografts, an observation consistent with previous data on MDA-MB-453 showing poor tumorigenic properties.[25] Of note, the difference in vascular density between MDA-MB-453 and MDA-MB-231 was in line with the observed differences in nanoparticle uptake, as only 3% of the total fluorescence were recovered in MDA-MB-453 xenografts, whereas up to 15% were found in MDA-231 xenografts, both figures to be compared with the $<0.1\%$ of T-DM1 recovered in tumors according to previous reports.[26] It is noteworthy that by our conditions spheroids were not able to predict T-DM1 efficacy on MDA-MB-453 cells, whereas the drug proved to reduce tumor growth by 100% in mice. It is not possible to explain this complete lack of transposition between in vitro and in vivo results with T-DM1, especially since conversely, differences in efficacy between immunoliposomes, free drugs, and liposomal docetaxel plus trastuzumab observed on spheroids remarkably matched the in vivo results. Developing immunoliposomes with taxane drugs in Her2+ breast cancer is a long story, with mixed results. Liposomal paclitaxel coated with trastuzumab already showed promising activity both in vitro and in vivo, but failed to be effective in the triple-negative MDA-MB-231 model as we observed.[27] More recently, a double encapsulation (paclitaxel and anti-mTor rapamycin) liposomal form coated with trastuzumab showed significant activity in tumor bearing animals, but unfortunately no comparison with the reference T-DM1 or trastuzumab-based regimen in Her2+ breast cancer was proposed, as we did.[28] Our data suggest that spheroids could be of major interest when prototyping nanoparticles, and that stealth immunoliposomes combining anti-Her2 trastuzumab and docetaxel are more efficacious than the currently approved treatments (ie, T-DM1 or trastuzumab + docetaxel combo) in breast cancer, regardless of Her2 expression.

Conclusion

In this work, we have demonstrated the feasibility of using 3D spheroid models, enabling a better and more accurate prediction of in vivo efficacy than standard 2D models. Several culturing conditions (ie, cell type, spheroid density, treatment scheduling, and dosing) were tested, thus highlighting their importance when translating into in vivo situations. In vitro and in vivo studies demonstrated that higher efficacy could be achieved with immunoliposomes when compared to reference treatments (ie, free docetaxel + trastuzumab or T-DM1), probably because of better drug delivery based upon passive and active targeting.

Acknowledgments

We thank Ligue Contre le Cancer for generously offering a grant to Anne Rodallec. Additionally, we thank the French Institut Roche who partly supported this study and Genentech who kindly provided trastuzumab.

Author contributions

AR, GS, RF, JC, SG, MC, and BP performed the bench experiments. AR, RF, and JC performed statistical analyses. AR, RF, BL, AS, FB, and JC wrote the manuscript. All authors contributed toward data analysis, drafting and revising the paper, and agree to be accountable for all aspects of the work.

Disclosure

AS and FB are members of Institut Roche, a joint institute from Roche Laboratories that commercializes trastuzumab and has partly funded this study. JC and RF obtained fees as board members of Roche. The other authors report no conflicts of interest in this work.

References

1. Becker S. A historic and scientific review of breast cancer: The next global healthcare challenge. *Int J Gynaecol Obstet*. 2015;131 Suppl 1: S36–S39.
2. Slamon DJ, Clark GM, Wong SG, Levin WJ, Ullrich A, McGuire WL. Human breast cancer: correlation of relapse and survival with amplification of the HER-2/neu oncogene. *Science*. 1987;235(4785): 177–182.
3. Sadeghi S, Olevsky O, Hurvitz SA. Profiling and targeting HER2-positive breast cancer using trastuzumab emtansine. *Pharmgenomics Pers Med*. 2014;7:329–338.
4. Marty M, Cognetti F, Maraninchi D, et al. Randomized phase II trial of the efficacy and safety of trastuzumab combined with docetaxel in patients with human epidermal growth factor receptor 2-positive metastatic breast cancer administered as first-line treatment: the M77001 study group. *J Clin Oncol*. 2005;23(19):4265–4274.
5. Rodallec A, Fanciullino R, Lacarelle B, Ciccolini J. Seek and destroy: improving PK/PD profiles of anticancer agents with nanoparticles. *Expert Rev Clin Pharmacol*. 2018;11(6):599–610.
6. Rodallec A, Brunel JM, Giacometti S, et al. Docetaxel-trastuzumab stealth immunoliposome: development and in vitro proof of concept studies in breast cancer. *Int J Nanomedicine*. 2018;13:3451–3465.
7. Kijanska M, Kelm J. In vitro 3D spheroids and microtissues: ATP-based cell viability and toxicity assays. In: Sittampalam GS, editor. *Assay Guidance Manual*. Bethesda, MD: Eli Lilly & Company and the National Center for Advancing Translational Sciences; 2004. Available from: http://www.ncbi.nlm.nih.gov/books/NBK343426/. Accessed May 25, 2018.
8. Rodallec A, Benzekry S, Lacarelle B, Ciccolini J, Fanciullino R. Pharmacokinetics variability: Why nanoparticles are not just magic-bullets in oncology. *Crit Rev Oncol Hematol*. 2018;129:1–12.
9. Roth A, Singer T. The application of 3D cell models to support drug safety assessment: opportunities & challenges. *Adv Drug Deliv Rev*. 2014;69–70:179–189.
10. Yang T, Choi MK, Cui FD, et al. Preparation and evaluation of paclitaxel-loaded PEGylated immunoliposome. *J Control Release*. 2007;120(3):169–177.
11. Choi WI. "Targeted antitumor efficacy and imaging via multifunctional nano-carrier conjugated with anti-HER2 trastuzumab," Nanomedicine: Nanotechnology. *Biol Med*. 2015;11(2):359–368.
12. Soema PC, Willems GJ, Jiskoot W, Amorij JP, Kersten GF. Predicting the influence of liposomal lipid composition on liposome size, zeta potential and liposome-induced dendritic cell maturation using a design of experiments approach. *Eur J Pharm Biopharm*. 2015;94:427–435.
13. Garg MB, Ackland SP. Simple and sensitive high-performance liquid chromatography method for the determination of docetaxel in human plasma or urine. *J Chromatogr B Biomed Sci Appl*. 2000;748(2): 383–388.
14. Bradford MM. A rapid and sensitive method for the quantitation of microgram quantities of protein utilizing the principle of protein-dye binding. *Anal Biochem*. 1976;72:248–254.
15. Carter PJ, Lazar GA. Next generation antibody drugs: pursuit of the 'high-hanging fruit'. *Nat Rev Drug Discov*. 2018;17(3):197–223.
16. Maeda H. The enhanced permeability and retention (EPR) effect in tumor vasculature: the key role of tumor-selective macromolecular drug targeting. *Adv Enzyme Regul*. 2001;41(1):189–207.
17. Bregoli L. "Nanomedicine applied to translational oncology: A future perspective on cancer treatment," Nanomedicine: Nanotechnology. *Biol Med*. 2016;12(1):81–103.
18. Godugu C, Patel AR, Desai U, Andey T, Sams A, Singh M. AlgiMatrix™ Based 3D Cell Culture System as an In-Vitro Tumor Model for Anticancer Studies. *PLoS One*. 2013;8(1):e53708.
19. Guo L, Zhou Y, Wang S, Wu Y. Epigenetic changes of mesenchymal stem cells in three-dimensional (3D) spheroids. *J Cell Mol Med*. 2014; 18(10):2009–2019.
20. Sha H, Zou Z, Xin K, et al. Tumor-penetrating peptide fused EGFR single-domain antibody enhances cancer drug penetration into 3D multicellular spheroids and facilitates effective gastric cancer therapy. *J Control Release*. 2015;200:188–200.
21. Lal-Nag M. Exploring drug dosing regimens in vitro using real-time 3d spheroid tumor growth assays. *SLAS Discov*. 2017;22:537–546.
22. Hare JI, Lammers T, Ashford MB, Puri S, Storm G, Barry ST. Challenges and strategies in anti-cancer nanomedicine development: An industry perspective. *Adv Drug Deliv Rev*. 2017;108:25–38.
23. Fanciullino R, Mollard S, Correard F, et al. Biodistribution, tumor uptake and efficacy of 5-FU-loaded liposomes: why size matters. *Pharm Res*. 2014;31(10):2677–2684.
24. Kirpotin DB, Drummond DC, Shao Y, et al. Antibody targeting of long-circulating lipidic nanoparticles does not increase tumor localization but does increase internalization in animal models. *Cancer Res*. 2006;66(13):6732–6740.
25. Holliday DL, Speirs V. Choosing the right cell line for breast cancer research. *Breast Cancer Res*. 2011;13(4):215.
26. Erickson HK, Lewis Phillips GD, Leipold DD, et al. The effect of different linkers on target cell catabolism and pharmacokinetics/pharmacodynamics of trastuzumab maytansinoid conjugates. *Mol Cancer Ther*. 2012;11(5):1133–1142.
27. Yang T, Choi MK, Cui FD, et al. Antitumor effect of paclitaxel-loaded PEGylated immunoliposomes against human breast cancer cells. *Pharm Res*. 2007;24(12):2402–2411.
28. Eloy JO, Petrilli R, Chesca DL, Saggioro FP, Lee RJ, Marchetti JM. Anti-HER2 immunoliposomes for co-delivery of paclitaxel and rapamycin for breast cancer therapy. *Eur J Pharm Biopharm*. 2017;115:159–167.